



Keloid-derived keratinocytes exhibit an abnormal gene expression profile consistent with a distinct causal role in keloid pathology

Jennifer M. Hahn, BS¹; Kathryn Glaser, BA¹; Kevin L. McFarland, MS, JD¹; Bruce J. Aronow, PhD²; Steven T. Boyce, PhD^{1,3}; Dorothy M. Supp, PhD^{1,3}

1. Research Department, Shriners Hospitals for Children—Cincinnati,
2. Department of Pediatrics, Division of Biomedical Informatics, Cincinnati Children's Hospital Medical Center, and
3. Department of Surgery, College of Medicine, University of Cincinnati, Cincinnati, Ohio, USA

Reprint requests:

Dr. D. M. Supp, Research Department,
Shriners Hospitals for Children—Cincinnati,
3229 Burnet Avenue, Cincinnati, OH
45229, USA.
Tel: +1 513 872 6346;
Fax: +1 513 872 6072;
Email: dsupp@shrinersnet.org

Manuscript received: September 5, 2012
Accepted in final form: March 18, 2013

DOI:10.1111/wrr.12060

ABSTRACT

Keloids are disfiguring scars that extend beyond the original wound borders and resist treatment. Keloids exhibit excessive extracellular matrix deposition, although the underlying mechanisms remain unclear. To better understand the molecular basis of keloid scarring, here we define the genomic profiles of keloid fibroblasts and keratinocytes. In both cell types, keloid-derived cells exhibit differential expression of genes encompassing a diverse set of functional categories. Strikingly, keloid keratinocytes exhibited decreased expression of a set of transcription factor, cell adhesion, and intermediate filament genes essential for normal epidermal morphology. Conversely, they exhibit elevated expression of genes associated with wound healing, cellular motility, and vascular development. A substantial number of genes involved in epithelial–mesenchymal transition were also up-regulated in keloid keratinocytes, implicating this process in keloid pathology. Furthermore, keloid keratinocytes displayed significantly higher migration rates than normal keratinocytes *in vitro* and reduced expression of desmosomal proteins *in vivo*. Previous studies suggested that keratinocytes contribute to keloid scarring by regulating extracellular matrix production in fibroblasts. Our current results show fundamental abnormalities in keloid keratinocytes, suggesting they have a profoundly more direct role in keloid scarring than previously appreciated. Therefore, development of novel therapies should target both fibroblast and keratinocyte populations for increased efficacy.

Keloids are an extreme form of excessive scarring that result from an abnormal wound healing process in susceptible individuals. Unlike normal scars, which stabilize with time after wound closure, keloids can increase in size indefinitely and spread beyond the original wound margin, resulting in significant morbidity due to decreased range of motion, pain, itching, and impaired self-image and quality of life. Keloids are extremely refractory to treatment, and despite a wide range of treatment modalities, recurrence is relatively common.¹ Keloids are characterized by excessive deposition of extracellular matrix (ECM), which is likely due to an imbalance of ECM production and degradation. Although the root cause of keloid scarring is not yet known, progress has been made in understanding keloid pathology at the cellular and molecular levels. Growth factors that regulate fibroblast activity, such as transforming growth factor- β (TGF- β) and epidermal growth factor (EGF), and their downstream signaling pathways have been implicated in dermal fibrosis and keloid scarring.^{2,3} Linkage analyses have identified multiple chromosomal loci associated with the risk for keloid formation, suggesting that there are likely many different genes or gene combinations involved.⁴

In normal wound healing, feedback mechanisms are in place that permit transition from the proliferative phase to the maturation phase upon wound closure, and it has been pro-

posed that excessive fibroblast proliferation and ECM production in keloid scars is due to an inability to respond to this feedback mechanism.² This implies that the abnormality resides in the fibroblast population, but keratinocytes have also been shown to play a role in keloid scarring through paracrine regulation of fibroblast function. For example, fibroblasts co-cultured with keloid keratinocytes display increased proliferation and elevated levels of collagen.⁵

To further elucidate the roles of keratinocytes and fibroblasts in keloid scarring, genomic profiling of keloid-derived cells and bioinformatics analyses were performed. Gene expression profiling of keloid keratinocytes, in addition to keloid fibroblasts, revealed abnormal expression of a large number of genes not previously implicated in keloid scarring. The results suggest that factors intrinsic to keloid keratinocytes play an active role in the excessive healing characteristic of keloid scars.

METHODS

Patient samples

Skin and scar samples used for isolation of primary keratinocytes and fibroblasts are listed in Table 1. Excised keloid

Table 1. Tissue samples used for isolation of primary keratinocytes and fibroblasts and analysis. Except where indicated (#), keloid scars were from burn survivors. Normal skin samples were from healthy nonburned donors. As indicated, cells from different strains were used for analysis by microarray, validation of expression levels using qRT-PCR, or migration analysis using an in vitro wound healing “scratch assay.” In addition, RNA was isolated from some intact keloid scars or normal human skin samples (“native tissue”) for qRT-PCR analysis

Gender	Age (years)	Ethnicity	Site	Cell strain #	Tissue source			Analysis of cells				
					Keloid	Adjacent to keloid	Normal	Microarray	qRT-PCR	Scratch assay	Native tissue qRT-PCR	
F	17	AA	Neck	744*	X			X				
F	20	AA	Neck	795*	X	X					X	
M	10	AA	Ear	758-1**	X			X				
			Face cheek	758-2**	X			X				
M	15	AA	Face	746	X	X		X			X	
M	11	C	Chin	753	X	X		X				
M	8	C	Ear	752	X			X				X
M	17	C	Ear	798	X			X			X	X
M	10	C	Ear	797	X	X		X			X	X
M	8	C/NA	Ear	817	X			X				X
F	12	AA	Ear	829#	X			X			X	X
M	3	AA	Ear	827	X			X			X	X
M	16	AA	Eyebrow	818-3\$	X			X			X	
M	17	AA	Face	823-2\$	X			X			X	X
M	17	AA	Neck	830-1**\$	X			X			X	X
			Ear	830-3**\$	X			X			X	X
M	9	AA	Ear	832	X			X			X	X
F	17	AA	Breast	793			X				X	
M	23	C	Torso	594***			X				X	
F	16	AA	Breast	737			X				X	
M	25	AA	Abdomen	766			X				X	
F	24	AA	Breast	811			X				X	
F	30	C	Abdomen	767			X				X	
F	17	C	Breast	815			X				X	
F	40	AA	Breast	806			X				X	X
F	38	C	Breast	831			X				X	X
F	30	Un	Breast	833			X				X	X

*Both tissue samples from keloid at same site on same patient; scar recurred and was reexcised.

**Multiple scars from different sites on single patient, excised during the same surgical procedure.

***Cadaveric donor.

\$Scars excised from same patient; different sites removed at different times after initial injury.

#This was the only nonburn keloid patient; recurrent scar resulting from ear piercing.

F, female; M, male; AA, African American; C, Caucasian; NA, Native American; Un, unknown.

scar samples were obtained with University of Cincinnati Institutional Review Board's approval and informed consent and according to Declaration of Helsinki principles, from pediatric and young adult patients undergoing elective scar excision surgeries at the Shriners Hospitals for Children—Cincinnati. Efforts were made to include a variety of keloid scars from different body sites, as well as both males and females and different ethnic backgrounds. For some patients, adjacent nonlesional skin samples were also obtained for establishment of primary cultures. These skin samples were available due to wide excision of the keloid scar such that adjacent tissue was also removed but was judged to be nonscar tissue by the surgeon performing the procedure. Additional nonkeloid skin biopsies were not collected from these patients due to ethical concerns regarding the risk of new keloid scar formation at the donor site. Normal skin samples were isolated from patients undergoing elective plastic surgery procedures at hospitals affiliated with the University of Cincinnati Medical Center, or from a cadaveric donor obtained through the Ohio Valley Tissue and Skin Center.

Cell culture

Primary cultures of keratinocytes and fibroblasts were prepared as described in detail elsewhere.⁶ Briefly, normal full-thickness skin samples, or samples of excised keloid scars, were incubated overnight at 4 °C in Dispase II (Roche Applied Science, Indianapolis, IN) to separate dermis from epidermis. Fibroblasts were isolated by finely mincing the dermal components followed by collagenase digestion (Worthington Biochemical Corp., Lakewood, NJ), and keratinocytes were released from epidermis using 0.025% trypsin (Sigma-Aldrich, St. Louis, MO). Fibroblasts were cultured in Dulbecco's modified Eagle's medium (Life Technologies, Carlsbad, CA) supplemented with 10 ng/mL EGF (Pepro-Tech, Rocky Hill, NJ), 5 µg/mL insulin (Life Technologies), 0.5 µg/mL hydrocortisone (Sigma-Aldrich), 0.1 mM ascorbic acid-2-phosphate (AA2P; Sigma-Aldrich), 4% fetal bovine serum (Life Technologies), and 1X Penicillin-Streptomycin-Fungizone (PSF; Life Technologies). Primary keratinocyte cultures were initiated using tissue culture flasks coated with collagen (Coating Matrix; Life Technologies), in medium containing reduced calcium (0.06 mM CaCl₂). Keratinocyte medium consisted of MCDB153, prepared in the investigators' laboratories, supplemented with 0.2% bovine pituitary extract, 1 ng/mL EGF, 5 µg/mL insulin, 0.5 µg/mL hydrocortisone, 0.1 mM AA2P, and 1X PSF. After subculture of primary keratinocytes, collagen coating was discontinued, and the CaCl₂ was increased to 0.2 mM. All cells were subcultured or harvested for analysis when they reached approximately 80–90% confluence to prevent contact inhibition and differentiation. Cells were analyzed up to passage 3.

Microarray analysis and bioinformatics

Cells from nine keloid scars, four adjacent nonlesional keloid patient skin samples, and three normal skin samples were analyzed using expression microarrays. RNA was isolated (RNeasy kit; Qiagen, Valencia, CA), and the quality was verified using an Agilent 2100 Bioanalyzer (Agilent Technologies, Inc., Wilmington, DE). Labeling and hybridization to Affymetrix Human Gene 1.0 ST microarray chips (Affyme-

trix Inc., Santa Clara, CA) were performed by the Vanderbilt Genome Sciences Resource at Vanderbilt University Medical Center (Nashville, TN). CEL files were generated using Expression Console v1.1.1 (Affymetrix) and subjected to robust multiarray averaging (RMA) normalization using Affymetrix CDF probe definitions and GeneSpringGX v7.3.1 (Agilent). The entire data set is available online at <http://www.ncbi.nlm.nih.gov/geo/> (accession #GSE44270). The relative expression levels for each probeset were calculated by normalization to the median value for all 32 samples analyzed, including all fibroblast and keratinocyte samples. Probesets with raw expression values greater than 150 for any two samples were selected for further analyses. Statistical analysis using analysis of variance (ANOVA) identified probesets that showed statistically significant expression differences between groups (keloid, adjacent nonlesional, and normal) with less than 5% false discovery using Benjamini Hochberg *p*-value correction based on a Student's *t* test. This resulted in a list of 1,311 probesets in fibroblasts and 1,758 probesets in keratinocytes that were differentially expressed among the three groups. Further dissection of this large data set was performed to limit the detailed analysis to probesets showing a greater than 1.3-fold difference in relative expression between normal and keloid cells. This resulted in a list of 462 probesets total, 264 in fibroblasts and 216 in keratinocytes that were at least 1.3-fold increased or decreased in keloid cells relative to normal cells, with a corrected *p*-value <0.05 (Supplemental Figures S1 and S2). Probesets that were specific to pseudogenes or to sequences no longer present in databases were removed from further analyses. ToppCluster⁷ (<http://toppcluster.cchmc.org/>) was used to identify functional enrichments in the fibroblast and keratinocyte gene lists, including relevant biological processes, pathways, and structures. The genes most highly expressed in the keloid keratinocyte gene list were further analyzed using Cytoscape⁸ (<http://www.cytoscape.org/>) to permit visualization of an integrated network of gene and pathway interactions.

Quantitative reverse transcription polymerase chain reaction (qRT-PCR)

Validation of expression of selected genes was performed using qRT-PCR, using different RNA samples than those used for microarray analysis. For validation purposes, fresh RNA samples were isolated from additional cultures of the same donor strains used for microarray analysis and from new keratinocyte and fibroblast cultures established from keloid scar and normal skin of additional donors, as indicated in Table 1. RNA was isolated (Qiagen RNeasy kit), and cDNA was prepared using the SuperScript VILO cDNA Synthesis kit (Life Technologies). Amplification was performed using gene-specific primers (RT² qPCR Primer Assays; Qiagen) and the iCycler iQ system (Bio-Rad, Hercules, CA). Fold differences between the glyceraldehyde 3-phosphate dehydrogenase (GAPDH) housekeeping gene and genes of interest were calculated as previously described.⁶ All qRT-PCR experiments were performed in technical triplicates in addition to biological replicates.

In vitro wound healing and proliferation assays

Keratinocytes were inoculated at 1e5/cm² into 6-well multiwell plates (Corning, Corning, NY) coated with collagen

(Coating Matrix; Life Technologies) and were incubated in fully supplemented media for 18–24 hours, resulting in a confluent monolayer. A total of 10 cells strains, three normal and seven keloid, were analyzed in triplicate wells. Wounds were created by scratching the surface of each cell monolayer with a sterile 200 μ L pipette tip. Digital photographs were taken using phase-contrast microscopy at the time of wounding (time 0) and at 4, 8, 12, and 16 hours after wounding. Three microscopic fields were photographed per well, for a total of nine fields per cell strain per time point; these fields were etched using a 6-mm biopsy punch on the plates so that photographs were taken of the same regions at each time point. Image analysis (NIS-Elements AR3.1; Nikon, Melville, NY) was used to calculate the open area of each microscopic field, and these values were used to calculate % closure. Mean % closure values for each strain at each time point were averaged; statistical analysis utilized a two-way ANOVA (one factor repetition) and multiple pairwise comparisons utilized the Holm-Sidak method (SAS software; SAS, Cary, NC).

Proliferation of normal (strains 766, 767, and 811) and keloid (strains 746, 758-2, and 798) keratinocytes was measured by MTT (3-[4, 5-dimethylthiazol-2-yl]-2, 5-diphenyltetrazolium bromide; Sigma-Aldrich) assay. Cells were inoculated at $2.5 \times 10^4/\text{cm}^2$ into 24-well plates, four wells per strain, and were assayed after 48 hours of culture in supplemented growth medium, prior to reaching confluence. Absorbance was measured at 570 nM. Results for normal and keloid keratinocytes were compared by *t*-test.

Immunohistochemistry

Skin and keloid biopsies were frozen without fixation in M1 Embedding Matrix (Lipshaw, Pittsburgh, PA) for cryosectioning and were fixed in methanol and dried in acetone. Primary antibodies for immunohistochemistry included Mouse anti-JUP (Abgent, San Diego, CA) and Rabbit anti-PKP1 (Santa Cruz Biotechnology, Inc., Dallas, TX), and detection utilized the Vectastain ABC-Alkaline Phosphatase Universal Kit with ImmPact NovaRed Peroxidase Substrate (Vector Laboratories, Burlingame, CA). Primary antibody was omitted for negative controls.

Western blot analysis

Western blotting was used to quantify KRT7 and KRT1 protein levels in keratinocytes. Briefly, protein was isolated using the Mammalian Cell Lysis Kit (Sigma-Aldrich) from harvested cells using mechanical disruption. Protein samples were separated on 1 mm NuPage Novex 10% Bis-Tris gels using NuPage MOPS SDS Buffer Kit (Life Technologies) under reducing conditions and were transferred to 0.2 μ m nitrocellulose membranes. Western blot detections were performed using Mouse Anti-Cytokeratin 7 (Abcam, Cambridge, MA) and the Western Breeze Chemiluminescent Anti-Mouse Kit (Life Technologies), or Rabbit Anti-Cytokeratin 1 (Abcam) and the ECL Prime Western Blotting Detection Reagent and ECL Peroxidase Labeled Anti-Rabbit Antibody (GE Healthcare Biosciences, Pittsburgh, PA). To control for protein loading, blots were stripped and stained for beta-actin using Rabbit Anti-Beta-Actin antibody (Abcam) and ECL reagents (GE Healthcare Biosciences). Signals were visualized and quantified using the Alpha Innotech FC2 (Pro-

teinSimple, Santa Clara, CA) image analysis and gel documentation system. For quantification, the relative intensity levels for each cell strain were calculated using the ratio of KRT1 or KRT7 to beta-actin staining and were normalized to the mean of the normal keratinocyte sample levels.

RESULTS AND DISCUSSION

Microarray analysis and validation of relative expression levels

Keloid fibroblasts and keratinocytes were isolated from tissue excised from varying body sites and from patients of different ages and races and were compared with cells isolated from nonlesional skin adjacent to keloid scars and normal skin (Table 1). The most highly up- or down-regulated genes in keloid fibroblasts and keratinocytes are listed in Tables 2 and 3, respectively. qRT-PCR was used to confirm expression of 24 genes in keratinocytes, fibroblasts, and intact keloid scar and normal skin tissue (Table 4). To increase the stringency of the analysis used for validation, RNA was newly prepared from fresh cultures of some of the donor strains analyzed by microarray, and additional donor strains were also analyzed (Table 1). Although the levels of expression for many of the genes analyzed were variable among samples, the majority of genes analyzed showed the same trends in qRT-PCR and microarray analyses.

Gene expression profiles of keloid scar cells and adjacent nonlesional cells

Many of the genes increased in keloid cells compared with normal cells were also increased in cells isolated from nonlesional skin adjacent to keloid scars (Figure 1). These similarities in gene expression may represent donor-specific differences related to keloid scar susceptibility. Alternatively, the observed expression patterns in adjacent nonlesional skin cells may reflect a gradient of expression from the central region of the keloid to the surrounding skin related to spreading of the active keloid into adjacent tissue.

One gene that was significantly decreased in keloid fibroblasts compared with nonlesional adjacent or normal fibroblasts is cannabinoid receptor 1 (CNR1) (Tables 2 and 4). This gene encodes one of two G-protein coupled receptors for cannabinoids, a group of lipids that includes Δ^9 -tetrahydrocannabinol as well as endogenous ligands, or endocannabinoids.⁹ The endocannabinoid system (ECS) was previously implicated in dermal fibrosis, including experimental models and the human fibrotic connective tissue disease systemic sclerosis.¹⁰ Furthermore, the ECS modulates several regulatory events in normal and cancer cells, including proliferation, apoptosis, angiogenesis, ECM production, cytokine expression, and inflammation.⁹

In keratinocytes, there were a limited number of genes that were specifically increased in keloid vs. nonlesional or normal cells (Table 5). These include four out of the five histone genes that were differentially expressed between keloid and normal keratinocytes, all encoding histone cluster 1 genes: HIST1H1A, HIST1H1B, HIST1H2BH, and HIST1H4F. Also specifically increased in keloid keratinocytes were the genes encoding the histone chaperone ASF1

Table 2. Genes differentially expressed >2.5-fold in keloid vs. normal fibroblasts

Symbol	Gene name	KF/NF	NLF/NF
POSTN	Periostin, osteoblast specific factor	10.95	4.21
SERPINB2	Serpin peptidase inhibitor, clade B (ovalbumin), member 2	5.50	1.55
EDIL3	EGF-like repeats and discoidin I-like domains 3	4.46	2.72
ABCC9	ATP-binding cassette, subfamily C (CFTR/MRP), member 9	3.51	1.83
SIX1	SIX homeobox 1	2.94	2.15
FGD4	FYVE, RhoGEF and PH domain containing 4	2.86	2.43
STC2	Stanniocalcin 2	2.82	1.83
CCND2	Cyclin D2	2.76	1.34
ENPEP	Glutamyl aminopeptidase (aminopeptidase A)	2.68	2.91
TMEM156	Transmembrane protein 156	2.65	2.27
DOK5	Docking protein 5	2.60	2.37
ZFX4	Zinc finger homeobox 4	2.54	1.69
CNR1	Cannabinoid receptor 1 (brain)	0.40	0.99
TFPI2	Tissue factor pathway inhibitor 2	0.38	0.45
MT1M	Metallothionein 1 M	0.37	0.50
AQP1	Aquaporin 1 (Colton blood group)	0.37	0.45
TRPA1	Transient receptor potential cation channel, subfamily A, member 1	0.36	0.36
TNC	Tenascin C	0.36	0.44
AQP9	Aquaporin 9	0.35	0.38
TRPV2	Transient receptor potential cation channel, subfamily V, member 2	0.35	0.36
DKK3	Dickkopf homolog 3 (<i>Xenopus laevis</i>)	0.35	0.46
HOXC8	Homeobox C8	0.33	0.26
SKAP2	Src kinase associated phosphoprotein 2	0.30	0.23
HOXC10	Homeobox C10	0.30	0.23
HOXA9	Homeobox A9	0.27	0.24

KF, keloid fibroblasts; NF, normal fibroblasts; NLF, nonlesional fibroblasts (adjacent to keloid).

anti-silencing function 1 homolog B (ASF1B) and centromere proteins K and H. The elevated expression of genes involved in chromatin organization and kinetochore structure suggest elevated mitotic rates in keloid keratinocytes. However, results of an MTT assay performed to compare proliferation in normal and keloid keratinocytes did not show significant differences: absorbance values were 0.817 ± 0.137 vs. 0.912 ± 0.192 , respectively.

Genomic profiling of keloid fibroblasts extends previous findings and identifies new expression abnormalities

In the current study, many of the genes differentially regulated in keloid vs. normal fibroblasts were previously implicated in keloid scarring. These include: periostin (POSTN), serpin peptidase inhibitor clade b member 2 (SERPINB2), SIX homeobox 1 (SIX1), cyclin D2 (CCND2), docking protein 5 (DOK5), tissue factor pathway inhibitor 2 (TFPI2), dickkopf homolog 3 (DKK3), and homeobox genes HOXC10 and HOXA9 (Table 2).^{6,11,12} The current study also identified several genes with diverse functions that were not previously implicated in keloid scarring (Table 2 and Supporting information Figure S1). Examples of genes increased in keloid

fibroblasts include EGF-like repeats and discoidin I-like domains 3 (EDIL3), an integrin-binding protein that promotes cell proliferation, adhesion, and migration;¹³ FYVE, RhoGEF and PH Domain Containing 4 (FGD4), a Rho GDP/GTP nucleotide exchange factor involved in regulating cell shape;¹⁴ and stanniocalcin 2, a secreted glycoprotein associated with tumor cell invasion, metastasis, and epithelial–mesenchymal transition (EMT).¹⁵ Among novel genes down-regulated in keloid fibroblasts are transient receptor potential cation channel, subfamily A, member 1 and subfamily V, Member 2 (TRPA1 and TRPV2). Genes of the TRP superfamily encode temperature-sensitive ion channels that were shown to be activated by cannabinoids.¹⁶ Along with decreased expression of the CNR1 gene in keloid fibroblasts, reduced TRPA1 and TRPV2 further implicates endocannabinoid signaling in keloid pathology.

Functional analysis of the keloid fibroblast expression profile

By examining patterns of coordinate gene expression, significant functional information and insight into the pathological process can be obtained. Pathways analysis of the fibroblast gene set (Supporting information Table S1) showed that the molecular function “transcription regulatory activity” was

Table 3. Genes differentially expressed >2-fold in keloid vs. normal keratinocytes

Symbol	Gene name	KK/NK	NLK/NK
HAS2	Hyaluronan synthase 2	4.38	3.01
KRT7	Keratin 7	3.52	4.85
GLIPR1	GLI pathogenesis-related 1	3.48	3.76
ANO1	Anoctamin 1, calcium activated chloride channel	3.00	2.50
LOXL2	Lysyl oxidase-like 2	2.79	2.13
ADAM19	ADAM metalloproteinase domain 19	2.74	3.11
LGALS1	Lectin, galactoside-binding, soluble, 1	2.66	2.84
ITGA4	Integrin, alpha 4 (antigen CD49D, alpha 4 subunit of VLA-4 receptor)	2.59	2.47
CDH11	Cadherin 11, type 2, OB-cadherin (osteoblast)	2.57	3.41
DAB2	Disabled homolog 2, mitogen-responsive phosphoprotein (Drosophila)	2.30	2.57
BCAT1	Branched chain amino-acid transaminase 1, cytosolic	2.20	2.36
VIM	Vimentin	2.07	2.28
BICC1	Bicaudal C homolog 1 (Drosophila)	2.07	2.06
ANPEP	Alanyl (membrane) aminopeptidase	2.00	3.62
PXDN	Peroxidasin homolog (Drosophila)	2.00	2.38
PLA2G4A	Phospholipase A2, group IVA (cytosolic, calcium-dependent)	0.50	0.48
C6orf105	Chromosome 6 open reading frame 105	0.48	0.55
GJB6	Gap junction protein, beta 6, 30kda	0.47	0.41
IGFL1	IGF-like family member 1	0.45	0.40
EPGN	Epithelial mitogen homolog (mouse)	0.44	0.57
SERPINB13	Serpin peptidase inhibitor, clade B (ovalbumin), member 13	0.42	0.41
HOXA7	Homeobox A7	0.41	0.35
ABCA12	ATP-binding cassette, sub-family A (ABC1), member 12	0.39	0.44
MMP3	Matrix metalloproteinase 3 (stromelysin 1, progelatinase)	0.39	0.57
KRT1	Keratin 1	0.38	0.27
STEAP4	STEAP family member 4	0.35	0.33
A2ML1	Alpha-2-macroglobulin-like 1	0.35	0.34
HOXA9	Homeobox A9	0.23	0.18
KRT31	Keratin 31	0.21	0.24
DSC1	Desmocollin 1	0.20	0.15
CRYAB	Crystallin, alpha B	0.19	0.20

KK, keloid keratinocytes; NK, normal keratinocytes; NLK, nonlesional keratinocytes (adjacent to keloid).

highly significant, with 27 genes up- or down-regulated in keloid vs. normal fibroblasts, including 15 HOX genes. It is not surprising, therefore, that “organ morphogenesis” was the most significant biological process associated with this gene set, followed by “regulation of cell proliferation” (Supporting information Table S1). The cellular component category most significantly represented in the genomic profile of keloid fibroblasts is “integral to plasma membrane,” which includes 31 genes encoding membrane glycoproteins, receptors, water channels, ion channels, membrane-associated enzymes, and integrins. Among significant pathways associated with the keloid fibroblast gene set were “O-glycan biosynthesis” and “altered canonical Wnt signaling.”

A diverse set of genes is differentially expressed in keloid vs. normal keratinocytes

Genomic profiling of keloid keratinocytes revealed a highly diverse gene set encoding many different types of proteins.

However, despite the observed variety, a common thread is that a large number of these genes have been implicated in differentiation, cell adhesion, migration, invasion, and EMT.

The hyaluronan synthase 2 (HAS2) gene, which encodes one of three HAS enzymes involved in biosynthesis of hyaluronan, was increased 4.38-fold in keloid keratinocytes (Table 3). Hyaluronan, a high molecular weight glycosaminoglycan, is an important component of the epidermal ECM.¹⁷ Elevated HAS2 expression in keloid keratinocytes is consistent with previous reports of increased hyaluronan levels in keloid epidermis.¹⁸ Like many of the other genes increased in keloid keratinocytes, described in detail below, elevated HAS2 expression has been implicated in cancer cell proliferation and metastasis,¹⁹ and overexpression resulted in increased keratinocyte migration *in vitro*.¹⁷

Keratin 7 (KRT7) was increased 3.52-fold in keloid vs. normal keratinocytes (Table 3). KRT7 is a low molecular weight type II keratin that is expressed in simple epithelial tissues, including glandular epithelia but not in normal

Table 4. Quantification of gene expression using qRT-PCR compared with microarray expression levels

Fibroblasts:		Relative expression by qRT-PCR: mean (range)		Microarray fold change	
Gene name	Normal fibroblasts	Keloid fibroblasts	(KF/NF)		
POSTN	1 (.46–1.92)	22.76 (1.39–81.09)	10.95		
SERPINB2	1 (0.38–2.91)	16.76 (1.13–45.46)	5.50		
CCND2	1 (.56–2.22)	6.11 (3.07–13.49)	2.76		
ZFH4	1 (0.24–2.04)	4.00 (2.88–5.76)	2.54		
PRICKLE1	1 (0.64–1.84)	4.71 (2.27–8.65)	2.29		
SERPINB7	1 (0.36–2.11)	7.74 (1.11–15.42)	2.08		
PXDN	1 (0.76–1.26)	2.33 (1.20–3.25)	1.67		
ADAMTS6	1 (0.57–1.34)	1.64 (1.06–2.62)	1.56		
IER3	1 (0.91–1.12)	1.88 (1.25–3.02)	1.45		
ADAM19	1 (0.58–1.59)	3.55 (1.71–6.68)	1.40		
AXIN2	1 (0.43–2.37)	0.63 (0.44–0.88)	0.76		
ANPEP	1 (0.73–1.36)	0.97 (0.60–1.33)	0.74		
HOXC11	1 (0.66–4.02)	0.02 (0–0.1)	0.60		
HOXA7	1 (0.81–1.29)	0 (0–0.01)	0.44		
CNR1	1 (0.54–1.43)	0.17 (0.06–0.29)	0.40		
HOXA9	1 (0.72–1.31)	0 (0–0.01)	0.27		
Keratinocytes:		Relative expression by qRT-PCR: mean (range)		Microarray fold change	
Gene name	Normal keratinocytes	Keloid keratinocytes	(KK/NK)		
HAS2	1 (0.18–5.24)	19.28 (2.03–60.71)	4.38		
KRT7	1 (0.36–4.36)	3.73 (0.74–9.78)	3.52		
LOXL2	1 (0.41–4.22)	2.26 (1.36–4.74)	2.79		
ADAM19	1 (0.56–2.8)	4.26 (2.44–10.68)	2.74		
CDH11	1 (0.23–4.31)	1.87 (0.76–4.31)	2.57		
ANPEP	1 (0.32–2.47)	1.42 (0.83–1.63)	2.00		
PXDN	1 (0.6–1.54)	1.47 (0.64–2.23)	2.00		
WNT5A	1 (0.75–1.57)	1.81 (1.47–2.33)	1.73		
ADAMTS6	1 (0.35–1.59)	1.44 (0.54–2.25)	1.66		
HOXC11	1 (0.49–1.87)	0.12 (0.01–0.42)	0.68		
TGFBR3	1 (0.27–1.68)	0.93 (0.64–1.19)	0.59		
WNT3	1 (0.65–1.89)	0.60 (0.31–2.12)	0.55		
SERPINB7	1 (0.75–2.27)	0.76 (0.62–0.94)	0.54		
SERPINB2	1 (0.43–3.98)	1.76 (1.34–2.4)	0.52		
HOXA7	1 (0.49–1.46)	0.11 (0.02–0.31)	0.41		
MMP3	1 (0.22–4.01)	0.72 (0.11–1.96)	0.39		
HOXA9	1 (0.86–1.68)	0.05 (0.01–0.15)	0.23		
Whole tissue:		Relative expression by qRT-PCR: mean (range)		Microarray fold change	
Gene name	Normal skin	Keloid scar	Fibro. (KF/NF)	Kerat. (KK/NK)	
POSTN	1 (0.57–1.52)	22.77 (4.02–57.28)	10.95	N/A	
PXDN	1 (0.57–1.43)	4.85 (1.84–8.06)	1.67	2.00	
ADAM19	1 (0.5–1.95)	3.58 (1.7–7.46)	1.40	2.74	
HOXC11	1 (0.39–2.09)	0.23 (0.00–0.63)	0.60	0.68	
HOXA7	1 (0.94–1.08)	0.23 (0.01–0.48)	0.44	0.41	
CNR1	1 (0.89–1.15)	0.86 (0.16–1.70)	0.40	N/A	
LOXL2	1 (0.87–1.18)	15.27 (1.70–40.32)	N/A	2.79	
CDH11	1 (0.83–1.15)	10.31 (2.14–17.96)	N/A	2.57	
TGFBR3	1 (0.84–1.17)	0.62 (0.25–1.37)	N/A	0.59	

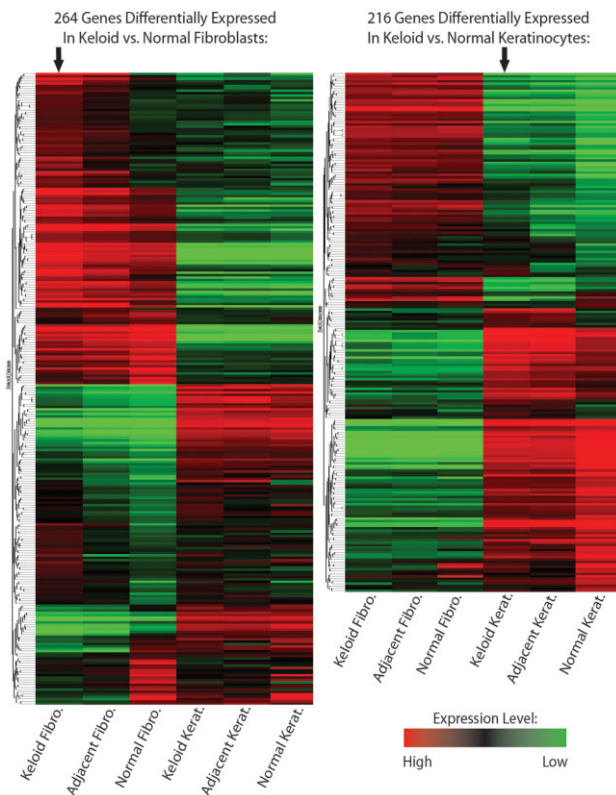


Figure 1. Relative expression levels of genes differentially expressed in keloid fibroblasts and keratinocytes. Shown are heat maps for 264 genes in fibroblasts (left) and 216 genes in keratinocytes (right) that were differentially expressed between keloid and normal cells. Rows represent individual genes, and columns represent the mean for each sample group. The complete gene lists corresponding to these gene trees are presented in Supporting information Figures S1 and S2. The heat maps permit visualization of the relative similarities and differences in expression profiles among the different sample types (cells from normal skin, skin adjacent to keloid, and keloid scar). Note that for each gene set, expression is illustrated for all samples, not just fibroblasts or keratinocytes.

epidermal keratinocytes.²⁰ KRT7 expression is often colocalized with KRT18,²⁰ which was also increased in keloid vs. normal keratinocytes (Supporting information Figure S2). KRT7 expression was found in a subset of colorectal cancers, where it was significantly associated with poor tumor differentiation and extensive tumor budding, with high KRT7 levels in single cells or clusters at the invasive tumor front.²¹ This *de novo* KRT7 was proposed to be related to the process of EMT. Furthermore, KRT7 expression was shown to be an indicator of metastatic potential in esophageal squamous cell carcinoma (SCC), where it was coexpressed with lysyl oxidase-like 2 (LOXL2).²² In keloid keratinocytes, LOXL2 was increased compared with normal keratinocytes (Tables 3 and 4). Lysyl oxidases are required for formation of cross-links in collagen and elastin. LOXL2 has been implicated in EMT, tumor progression, tumor cell invasion, and regulation of epidermal differentiation.²³ Silencing of LOXL2 gene expres-

sion in SCC cells resulted in reduced invasive potential and up-regulation of differentiation-specific genes,²³ suggesting the therapeutic potential of LOXL2 reduction for keloid suppression.

Consistent with reduced differentiation, keloid keratinocytes displayed reduced expression of KRT1 and KRT16 (Table 3 and Supporting information Figure S2). KRT1 is normally expressed in the spinous and granular epidermal layers of skin, and KRT16 is a marker of activated keratinocytes.²⁴ Increased KRT7 and decreased KRT1 protein levels were confirmed by Western blot analysis (Figure 2). The altered expression profile of keratin genes in keloid keratinocytes suggests reduced differentiation and increased migration.

Several mesenchymal cell markers were increased in keloid keratinocytes compared with normal keratinocytes, further implicating EMT in keloid scarring. For example, cadherin-11 (CDH11) and vimentin (VIM) were both increased in keloid keratinocytes (Tables 3 and 4). Cadherins function to mediate calcium-dependent cell–cell adhesion at adherens junctions, and VIM is an intermediate filament. Both are associated with a mesenchymal phenotype and are considered markers of EMT.²⁵ The process of EMT has been linked with fibrosis in diverse organ systems including lung, liver, and kidney, as well as skin.²⁶ The current studies suggest that EMT may also play a role in keloid fibrosis.

Functional analysis of keloid keratinocyte expression profile suggests decreased cell–cell adhesion and increased motility

The most significant molecular function associated with the keloid keratinocyte genomic profile was “structural molecule activity” (Supporting information Table S2). In addition to five keratin genes, this classification included the intermediate filament genes synemin (SYNM) and VIM; precursors of the cornified envelope envoplakin (EVPL) and cystatin A (CSTA); and desmosome components junction plakoglobin/gamma catenin (JUP) and plakophilin 1 (PKP1). EVPL and CSTA were both decreased in keloid keratinocytes compared with normal keratinocytes, consistent with reduced differentiation status. SYNM is decreased 1.59-fold in keloid keratinocytes; in previous studies, decreased SYNM expression was shown to interfere with cell adhesion and to increase cell migration.²⁷ JUP and PKP1 were both reduced in keloid keratinocytes; this reduction was validated in keloid tissue by immunohistochemistry, which showed reduced expression at cell–cell junctions (Figure 3). Reduced and abnormal localization of JUP and PKP1 suggest defects in desmosomal plaques of keloid keratinocytes. Mutations in JUP or PKP1 impact skin integrity and keratinocyte adhesion.²⁸

Another molecular function significantly associated with the keloid keratinocyte gene set was “frizzled binding.” Because frizzled (FZD) family members serve as receptors for secreted wingless-type MMTV integration site family (WNT) glycoproteins, this suggests altered Wnt/ β -catenin signaling, which was also revealed in analysis of the keloid fibroblast gene set (Supporting information Table S1) and previously described in keloid fibroblasts.^{29,30} Frizzled-7 (FZD7) and WNT5A were both increased in keloid keratinocytes. Wnt5A modulates cell movement and polarity, and its expression in different types of cancer contributes to an

Table 5. Genes differentially expressed in keloid keratinocytes compared with normal keratinocytes and adjacent nonlesional keratinocytes

Symbol	Gene name	Expression ratio	
		KK/NK	NLK/NK
HIST1H1A	Histone cluster 1, H1a	1.60	0.82
MOXD1	Monoxygenase, DBH-like 1	1.64	0.94
DLEU2	Deleted in lymphocytic leukemia 2 (nonprotein coding)	1.55	0.82
HIST1H4F	Histone cluster 1, H4f	1.46	0.86
MNS1	Meiosis-specific nuclear structural 1	1.44	0.95
HIST1H2BH	Histone cluster 1, H2bh	1.42	0.78
CENPK	Centromere protein K	1.39	0.82
CENPH	Centromere protein H	1.37	0.80
C4orf46	Chromosome 4 open reading frame 46	1.36	0.76
ZNF440	Zinc finger protein 440	1.36	0.98
CNTNAP3	Contactin associated protein-like 3	1.35	0.98
ASF1B	ASF1 anti-silencing function 1 homolog B (<i>S. cerevisiae</i>)	1.32	0.84
HIST1H1B	Histone cluster 1, H1b	1.31	0.64
BAMBI	BMP and activin membrane-bound inhibitor homolog (<i>Xenopus laevis</i>)	0.67	1.02

KK, keloid keratinocytes; NK, normal keratinocytes; NLK, nonlesional keratinocytes.

invasive and metastatic phenotype through induction of EMT.³¹ FZD7 is critical for normal development and is regarded as the most important WNT receptor in the development and progression of cancers of the breast, liver, and other organs.³²

“Biological adhesion” was the most significant biological process associated with the keloid keratinocyte gene set, with 27 genes either up- or down-regulated in keloid keratinocytes (Supporting information Table S2 and Table 6). These genes encode a diverse collection of proteins implicated in fibrosis, tumor progression, metastasis, and cell invasion, revealing potential mechanisms for suppression of keloid scarring by regulation of these processes. In particular, genes involved in EMT are enriched in this group, suggesting the importance of

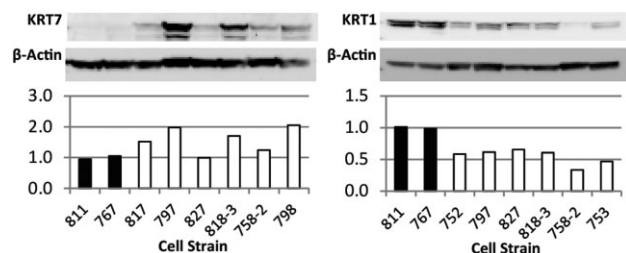


Figure 2. Expression of keratins 7 (KRT7) and 1 (KRT1) in normal and keloid keratinocytes. Western blot analysis of multiple cell strains ($n=2$ normal, 6 keloid) showing increased KRT7 (left) and decreased KRT1 (right) in keloid keratinocytes; beta-actin staining of blots was used to control for loading. Normalized expression levels were calculated by image analysis and are shown below the blot images. Protein levels varied between samples, but mean levels were increased for KRT7 and decreased for KRT1.

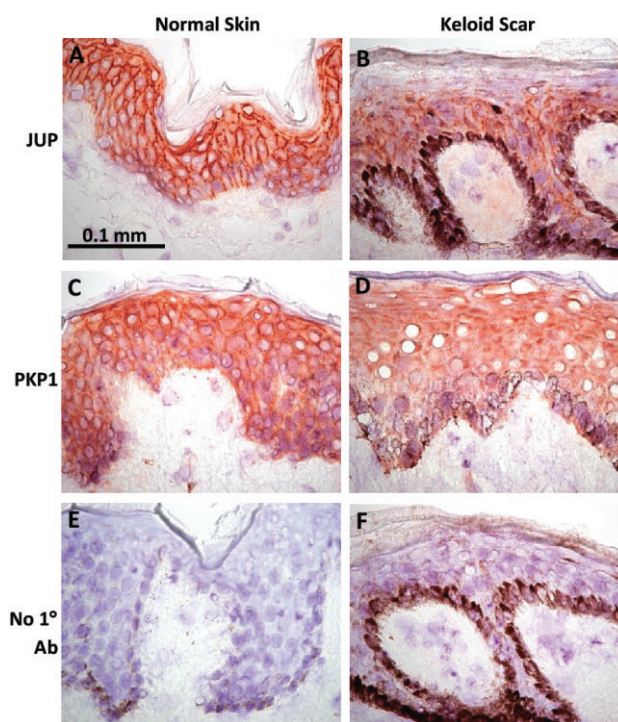


Figure 3. Localization of desmosome components junction plakoglobin (JUP) and plakophilin 1 (PKP1) in normal skin and keloid scar. In normal epidermis, JUP (A) and PKP1 (C) staining was localized to cell membranes (reddish-brown staining). In keloid epidermis, JUP (B) and PKP1 (D) staining levels were reduced, and membrane localization was absent or greatly decreased. Dark brown pigment in basal epidermal cells is due to melanin and is seen in negative controls stained without primary antibodies: normal skin (E) and keloid scar (F).

Table 6. Biological adhesion genes differentially expressed in keloid keratinocytes compared with normal keratinocytes; the ratio of normalized expression levels is shown

Symbol	Gene name	KK/NK
LOXL2	Lysyl oxidase-like 2	2.79
LGALS1	Lectin, galactoside-binding, soluble, 1	2.66
ITGA4	Integrin, alpha 4 (antigen CD49D, alpha 4 subunit of VLA-4 receptor)	2.59
CDH11	Cadherin 11, type 2, OB-cadherin (osteoblast)	2.57
AXL	AXL receptor tyrosine kinase	1.75
BVES	Blood vessel epicardial substance	1.74
WNT5A	Wingless-type MMTV integration site family, member 5A	1.73
NRP1	Neuropilin 1	1.71
NRP2	Neuropilin 2	1.64
AMIGO2	Adhesion molecule with Ig-like domain 2	1.58
GNE	Glucosamine (UDP-N-acetyl)-2-epimerase/N-acetylmannosamine kinase	1.55
FZD7	Frizzled family receptor 7	1.53
COL12A1	Collagen, type XII, alpha 1	1.47
FEZ1	Fasciculation and elongation protein zeta 1 (zygin I)	1.47
CD99L2	CD99 molecule-like 2	1.42
MMP14	Matrix metalloproteinase 14 (membrane-inserted)	1.36
CNTNAP3	Contactin associated protein-like 3	1.35
ALCAM	Activated leukocyte cell adhesion molecule	1.33
DLG1	Discs, large homolog 1 (Drosophila)	1.32
JUP	Junction plakoglobin	0.75
LMO7	LIM domain 7	0.65
MTSS1	Metastasis suppressor 1	0.64
FLRT3	Fibronectin leucine rich transmembrane protein 3	0.63
DSC2	Desmocollin 2	0.60
PKP1	Plakophilin 1 (ectodermal dysplasia/skin fragility syndrome)	0.58
HOXA7	Homeobox A7	0.41
DSC1	Desmocollin 1	0.20

KK, keloid keratinocytes; NK, normal keratinocytes.

reduction of epithelial cell adhesion and increased keratinocyte motility in keloid scarring. Genes up-regulated in keloid keratinocytes with roles in biological adhesion include CDH11, described above, and integrin alpha-4 subunit, which was reported to facilitate binding of fibroblasts to fibronectin.³³ Also increased in keloid keratinocytes was galectin 1 (LGALS1), which was previously shown to be up-regulated at the protein level in keloid scar compared with normal skin.³⁴ Galectins modulate cell–cell and cell–matrix interactions and have been implicated in regulation of cell proliferation, apoptosis, migration, and adhesion.³⁵ LGALS1 was previously shown to interact with Neuropilin 1 (NRP1), a receptor for vascular endothelial growth factor (VEGF), to mediate adhesion and migration of endothelial cells.³⁵ In the current study, NRP1 and the related NRP2 were both increased in keloid keratinocytes. Furthermore, NRP1 and NRP2 were both shown to be coreceptors for TGF- β 1, and it was proposed that neuropilins may function to enhance TGF- β signaling.³⁶ Hypothetically, increased NRP1 and NRP2 enhance TGF- β signaling in keloid cells. Alternatively, because VEGF was implicated in keloid scarring,³⁷ increased expression of neuropilins may contribute to enhanced keloid angiogenesis.

In addition to JUP and PKP1, reduced expression of desmosome components desmocollins 1 and 2 was observed in keloid keratinocytes, consistent with reduced cell–cell adhesion and a migratory phenotype. Furthermore, keloid keratinocytes exhibit reduced expression of metastasis suppressor-1, a tumor suppressor gene previously shown to promote cell adhesion and inhibit metastasis.³⁸

Keloid keratinocytes display enhanced motility in vitro

Morphological differences were observed between keloid and normal keratinocytes during in vitro monolayer culture (Figure 4A). Normal keratinocytes remained in close contact with each other even at subconfluent densities, but keloid keratinocytes formed looser colonies that were more widely dispersed, suggesting increased motility. An in vitro scratch assay was performed using seven keloid and three normal keratinocyte strains to investigate cell migration following in vitro wounding. Keloid keratinocytes migrated significantly faster than normal keratinocytes (Figure 4B and C).

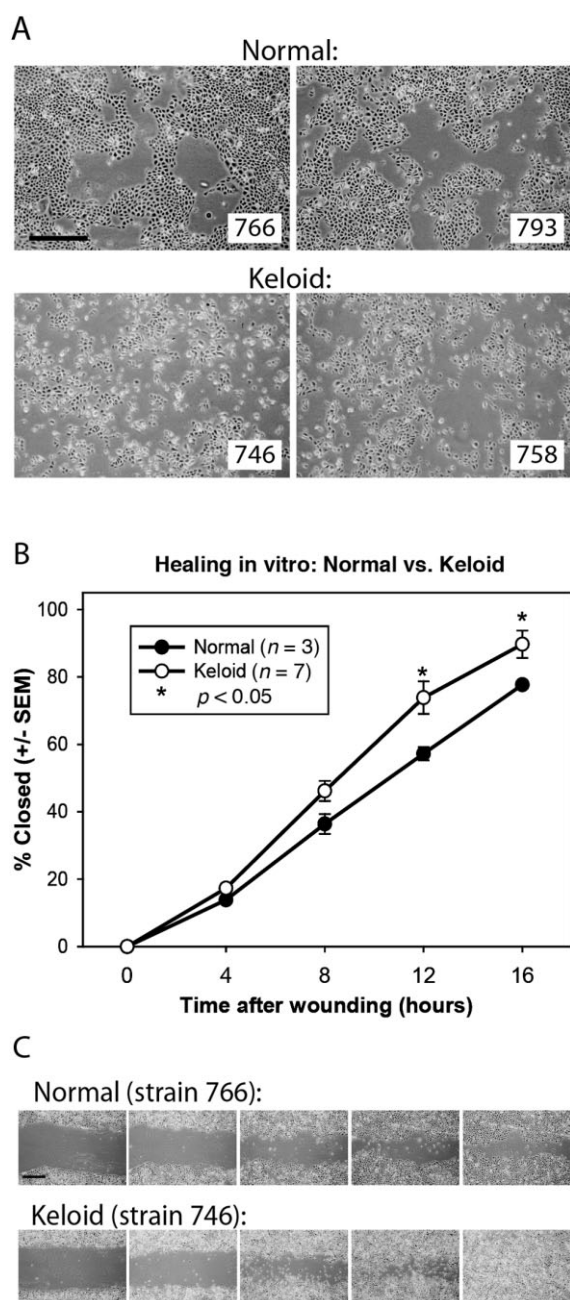


Figure 4. Increased motility in keloid keratinocytes. (A) Phase-contrast microscopy of normal and keloid keratinocytes, illustrating differences in morphology. Normal keratinocytes (top) maintain cell-cell contacts and form relatively tight colonies, whereas keloid keratinocytes (bottom) are more dispersed and display a migratory phenotype. Donor strain designations are indicated. Scale bar (500 μm) is the same for all panels. (B) Quantitative analysis of in vitro “healing” indicates that migration rates in keloid keratinocytes are significantly higher than in normal keratinocytes. Shown are mean values for % area closed at serial time points. (C) Representative phase-contrast images of “wounded” normal and keloid cultures. Scale bar (500 μm) is the same for all panels.

Network of interconnected genes differentially expressed in keloid vs. normal keratinocytes

To gain a more thorough understanding of the functional implications of the keloid keratinocyte gene expression profile, the functional analysis of selected genes up- and down-regulated in keloid keratinocytes was used to generate a graphic network (Figure 5). This network permits organization and visualization of the interconnectedness of the genes with each other and with significant functional categories. The network illustrates that genes down-regulated in keloid keratinocytes show functional enrichment for epidermal keratinization, differentiation, and cell junctions, and display gene expression patterns similar to stratified squamous nonkeratinized epithelia, such as the oral mucosa and esophagus. Genes up-regulated in keloid keratinocytes suggest significant involvement in cell adhesion, ECM, locomotion, and down-regulation of EGF receptor signaling. In addition to highlighting functional connectivity, the network highlights transcription factors that may be involved in regulation of the keloid expression pattern, as well as drugs that may be candidates for intervention in keloid pathology (Figure 5).

Genes common to both keloid fibroblast and keratinocyte gene sets

A small subset of genes was common to both keloid fibroblast and keratinocyte gene sets. Among these were three enzymes, peroxidase (PDXN), ADAM metalloproteinase domain 19 (ADAM19), and ADAM metalloproteinase with thrombospondin type 1 motif, 6 (ADAMTS6), which were increased in both keloid fibroblasts and keratinocytes compared with normal cells (Supporting information Figures S1 and S2). These enzymes all localize to the ECM but have not been previously described in skin or keloid scar. PDXN and ADAM19 were both previously implicated in fibrosis.^{39,40}

HOXA5, HOXA7, and HOXC11 were down-regulated in both keloid fibroblasts and keratinocytes. In total, nine different HOX genes were down-regulated in one or both keloid cell types (Supporting information Figures S1 and S2). Down-regulation of HOX expression in keloids has been previously reported.¹² HOX genes specify positional identity during embryonic development. They are differentially expressed along the anterior-posterior embryonic axis, and site-specific HOX gene expression in postnatal dermal fibroblasts was shown to be maintained in primary culture.⁴¹ Thus, it was suggested that the different body sites used for keloid and normal cell isolation might be responsible for differential HOX expression.¹² Alternatively, reduced HOX gene expression was proposed to be related to a “tumorigenic phenotype” of keloids, because many different HOX genes are misexpressed in cancer. HOX genes are known to be epigenetically regulated by both histone modifications and DNA methylation.⁴² Hypothetically, global keloid-specific epigenetic changes, which have been previously reported,²⁹ may result in HOX gene suppression in keloids, contributing to the fibrotic phenotype. Indeed, HOX gene down-regulation due to promoter methylation has been identified in multiple types of cancer compared with tissue-matched controls,⁴² supporting the notion that differential HOX gene expression observed here is functionally relevant and not an experimental artifact. Further functional and expression analyses comparing keloid

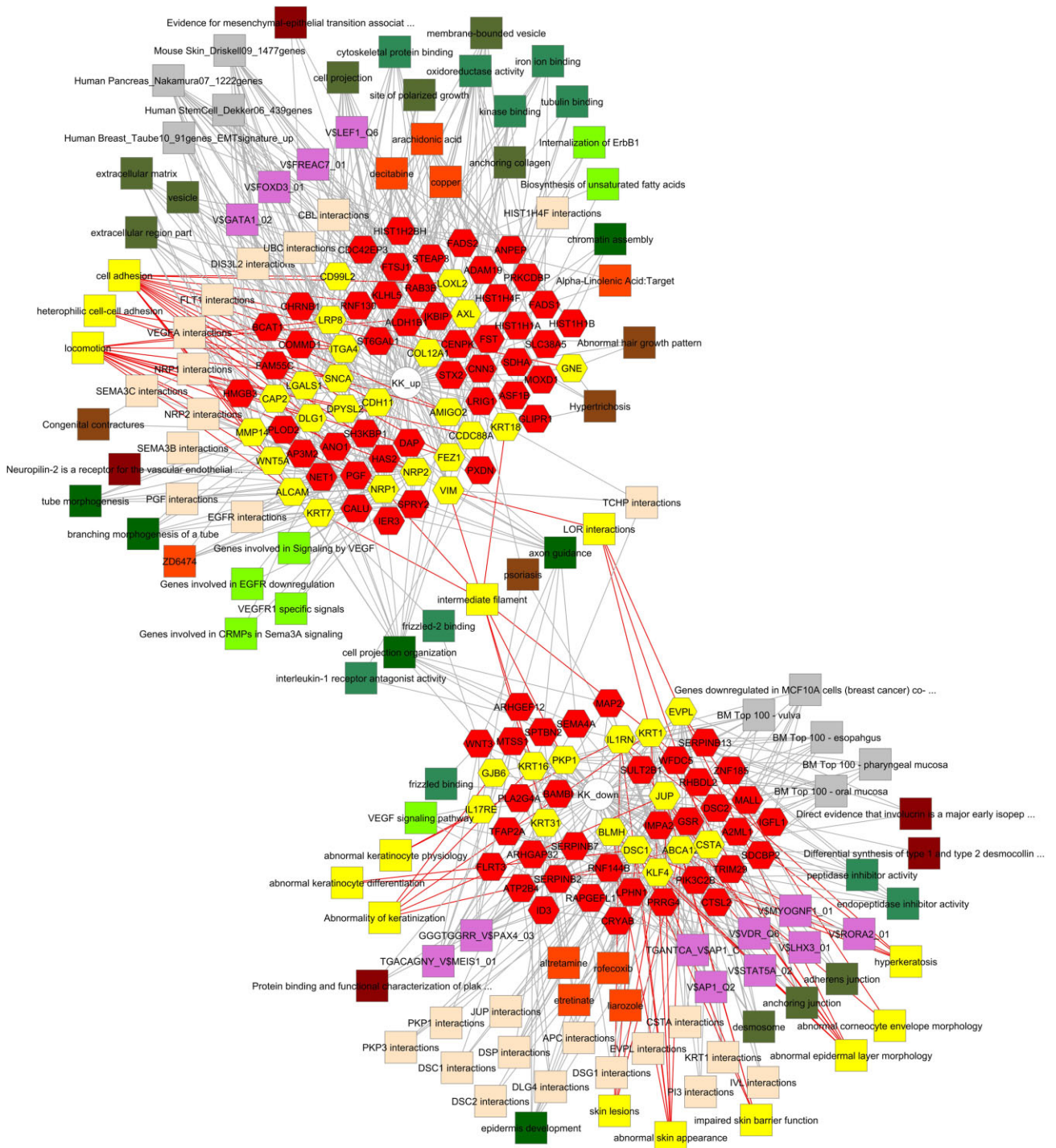


Figure 5. Network of gene interactions in keloid keratinocytes. Shown is a Cytoscape-generated network of genes and functional attributes, selected from analyses of genes increased (top left) or decreased (bottom right) in keloid vs. normal keratinocytes. Hexagons represent genes. Green or yellow squares represent annotated molecular functions, biological processes, cellular components, phenotypes, interactions, and pathways that are linked (red or gray lines) to genes in the keloid keratinocyte gene set. Other squares represent published expression studies (maroon), protein interactions (beige), transcription factor binding sites (purple), coexpression data (gray), human diseases (brown), and drugs (red). Highlighted in yellow are genes involved in keratinocyte differentiation, cell migration, and adhesion, linked by red lines to relevant functional attributes.

and normal skin samples from identical body sites will be required to resolve this issue.

CONCLUSIONS

This study is the first to characterize the expression profile of keloid keratinocytes in detail. The magnitude of the differences in mean expression levels between keloid and normal cells were, in many cases, relatively modest. There was substantial cell-type specific homogeneity between normal and keloid cells, with only 462 probesets differentially expressed greater than 1.3-fold in normal vs. keloid fibroblasts and keratinocytes. However, among those 462 probesets, there was considerable variability among keloid patient samples. Thus, the relatively modest fold changes may be due in part to variability, because a variety of keloid scar types was used, and also to the normalization scheme utilized, in which expression was normalized across all samples and both cell types. Hierarchical clustering and functional analysis can facilitate interpretation of such a complex data set. For example, if multiple genes involved in a particular pathway are similarly up- or down-regulated, the significance of that pathway in the disease process can be inferred, as in the current study. The results of the current study suggest that keloid keratinocytes are characterized by increased motility, decreased adhesion, and reduced differentiation compared with normal skin keratinocytes. These features, coupled with expression of mesenchymal cell markers, indicate that the process of EMT in keratinocytes may contribute to keloid scarring.

It has been suggested that keloids result from an inability to stop the wound healing process, in the context of increased or prolonged inflammation that increases dermal fibrosis.¹ Because excessive deposition of ECM is the hallmark of keloid scarring, fibroblasts have long been viewed as the critical cellular player. However, it now seems likely that keratinocytes help drive the continued growth that is characteristic of keloid scars, perhaps through the process of EMT.

Bioinformatics-based analysis of the keloid keratinocyte expression signature implicated multiple signaling pathways in keloid pathology that may be targeted for therapeutic intervention. Additionally, network analysis revealed potential candidate drugs that may be investigated in future studies for reducing pathology in keloid epidermis. A recent meta-analysis evaluated clinical studies aimed at keloid treatment, and the results indicated that high-quality evidence for many therapeutic interventions is lacking.⁴³ The majority of treatments strategies target the fibroblast population, including attempts to inhibit collagen production (intralesional steroid injection and interferon treatment), inhibit fibroblast proliferation (5-fluorouracil injection), or reduce inflammation-induced fibrosis (imiquimod).⁴³ These interventions may have had limited long-term success because they each address only one part of the problem and do not target keloid keratinocytes. Therefore, future studies must account for the central role of keratinocytes in keloid scarring for successful development of effective treatment and prevention strategies.

ACKNOWLEDGMENTS

The authors would like to thank Dr. Richard Kagan, Dr. Petra Warner, Dr. Kevin Bailey, Dr. Kevin Yakuboff, Dr. W. John

Kitzmilller, and Dr. Min-Doan Nguyen for assistance in obtaining surgical samples from patients and donors; the research nurses at Shriners Hospital for Children—Cincinnati (SHC-C), Mary Rieman, Laura Fowler, and Judy Nelson, for consenting patients and coordinating collection of samples; Deanna Leslie of the SHC-C Histology Core for preparation of histological specimens; and Rachel Zimmerman, Jill Pruszk, and William Kossenjans for their help with media preparation. We thank Dr. Rebekah Karns of the Bioinformatics Core at Cincinnati Children's Hospital Medical Center for critical review of the manuscript, and Laura James at SHC-C for statistical analysis of the *in vitro* assays. We are especially grateful for the generous cooperation of the patients at SHC-C and UC for donating their tissue for use in these studies.

Source of Funding: This work was supported by Research Grant #86200 from the Shriners Hospitals for Children.

Conflicts of Interest: The authors declare no conflicts of interest for this work.

REFERENCES

- Butler PD, Longaker MT, Yang GP. Current progress in keloid research and treatment. *J Am Coll Surg* 2008; 206: 731–41.
- Shih B, Garside E, McGrouther DA, Bayat A. Molecular dissection of abnormal wound healing processes resulting in keloid disease. *Wound Repair Regen* 2010; 18: 139–53.
- Satish L, Babu M, Tran KT, Hebda PA, Wells A. Keloid fibroblast responsiveness to epidermal growth factor and activation of downstream intracellular signaling pathways. *Wound Repair Regen* 2004; 12: 183–92.
- Shih B, Bayat A. Genetics of keloid scarring. *Arch Dermatol Res* 2010; 302: 319–39.
- Xia W, Phan TT, Lim IJ, Longaker MT, Yang GP. Complex epithelial-mesenchymal interactions modulate transforming growth factor-beta expression in keloid-derived cells. *Wound Repair Regen* 2004; 12: 546–56.
- Supp DM, Hahn JM, Glaser K, McFarland KL, Boyce S. Deep and superficial keloid fibroblasts contribute differentially to tissue phenotype in a novel *in vivo* model of keloid scar. *Plast Reconstr Surg* 2012; 129: 1259–71.
- Kaimal V, Bardes EE, Tabar SC, Jegga AG, Aronow BJ. ToppCluster: a multiple gene list feature analyzer for comparative enrichment clustering and network-based dissection of biological systems. *Nucleic Acids Res* 2010; 38: W96–102.
- Smoot ME, Ono K, Ruscheinski J, Wang PL, Ideker T. Cytoscape 2.8: new features for data integration and network visualization. *Bioinformatics* 2011; 27: 431–2.
- Biro T, Toth BI, Hasko G, Paus R, Pacher P. The endocannabinoid system of the skin in health and disease: novel perspectives and therapeutic opportunities. *Trends Pharmacol Sci* 2009; 30: 411–20.
- Servettaz A, Kaviani N, Nicco C, Deveaux V, Chereau C, Wang A, et al. Targeting the cannabinoid pathway limits the development of fibrosis and autoimmunity in a mouse model of systemic sclerosis. *Am J Pathol* 2010; 177: 187–96.
- Naitoh M, Kubota H, Ikeda M, Tanaka T, Shirane H, Suzuki S, et al. Gene expression in human keloids is altered from dermal to chondrocytic and osteogenic lineage. *Genes Cells* 2005; 10: 1081–91.
- Smith JC, Boone BE, Opalenik SR, Williams SM, Russell SB. Gene profiling of keloid fibroblasts shows altered expression in multiple fibrosis-associated pathways. *J Invest Dermatol* 2007; 128: 1298–310.

13. Wang Z, Kundu RK, Longaker MT, Quertermous T, Yang GP. The angiogenic factor Del1 prevents apoptosis of endothelial cells through integrin binding. *Surgery* 2012; 151: 296–305.
14. Delague V, Jacquier A, Hamadouche T, Poitelon Y, Baudot C, Boccaccio I, et al. Mutations in FGD4 encoding the Rho GDP/GTP exchange factor FRABIN cause autosomal recessive Charcot-Marie-Tooth type 4H. *Am J Hum Genet* 2007; 81: 1–16.
15. Law AY, Wong CK. Stanniocalcin-2 promotes epithelial-mesenchymal transition and invasiveness in hypoxic human ovarian cancer cells. *Exp Cell Res* 2010; 316: 3425–34.
16. De Petrocellis L, Orlando P, Moriello AS, Aviello G, Stott C, Izzo AA, Di Marzo V. Cannabinoid actions at TRPV channels: effects on TRPV3 and TRPV4 and their potential relevance to gastrointestinal inflammation. *Acta Physiol (Oxf)* 2012; 204: 255–66.
17. Rilla K, Lammi MJ, Sironen R, Torronen K, Luukkonen M, Hascall VC, et al. Changed lamellipodial extension, adhesion plaques and migration in epidermal keratinocytes containing constitutively expressed sense and antisense hyaluronan synthase 2 (Has2) genes. *J Cell Sci* 2002; 115: 3633–43.
18. Meyer LJ, Russell SB, Russell JD, Trupin JS, Egbert BM, Shuster S, et al. Reduced hyaluronan in keloid tissue and cultured keloid fibroblasts. *J Invest Dermatol* 2000; 114: 953–9.
19. Bernert B, Porsch H, Heldin P. Hyaluronan synthase 2 (HAS2) promotes breast cancer cell invasion by suppression of tissue metalloproteinase inhibitor 1 (TIMP-1). *J Biol Chem* 2011; 286: 42349–59.
20. Smith FJ, Porter RM, Corden LD, Lunny DP, Lane EB, McLean WH. Cloning of human, murine, and marsupial keratin 7 and a survey of K7 expression in the mouse. *Biochem Biophys Res Commun* 2002; 297: 818–27.
21. Harbaum L, Pollheimer MJ, Kornprat P, Lindtner RA, Schlemmer A, Rehak P, et al. Keratin 7 expression in colorectal cancer—freak of nature or significant finding? *Histopathology* 2011; 59: 225–34.
22. Sano M, Aoyagi K, Takahashi H, Kawamura T, Mabuchi T, Igaki H, et al. Forkhead box A1 transcriptional pathway in KRT7-expressing esophageal squamous cell carcinomas with extensive lymph node metastasis. *Int J Oncol* 2010; 36: 321–30.
23. Peinado H, Moreno-Bueno G, Hardisson D, Perez-Gomez E, Santos V, Mendiola M, et al. Lysyl oxidase-like 2 as a new poor prognosis marker of squamous cell carcinomas. *Cancer Res* 2008; 68: 4541–50.
24. Rugg EL, Leigh IM. The keratins and their disorders. *Am J Med Genet C Semin Med Genet* 2004; 131C: 4–11.
25. Strutz F, Zeisberg M, Ziyadeh FN, Yang CQ, Kalluri R, Muller GA, et al. Role of basic fibroblast growth factor-2 in epithelial-mesenchymal transformation. *Kidney Int* 2002; 61: 1714–28.
26. Thiery JP, Acloque H, Huang RY, Nieto MA. Epithelial-mesenchymal transitions in development and disease. *Cell* 2009; 139: 871–90.
27. Sun N, Huiatt TW, Paulin D, Li Z, Robson RM. Synemin interacts with the LIM domain protein zyxin and is essential for cell adhesion and migration. *Exp Cell Res* 2010; 316: 491–505.
28. Petrof G, Mellerio JE, McGrath JA. Desmosomal genodermatoses. *Br J Dermatol* 2012; 166: 36–45.
29. Russell SB, Russell JD, Trupin KM, Gayden AE, Opalenik SR, Nanney LB, et al. Epigenetically altered wound healing in keloid fibroblasts. *J Invest Dermatol* 2010; 130: 2486–96.
30. Sato M. Upregulation of the Wnt/beta-catenin pathway induced by transforming growth factor-beta in hypertrophic scars and keloids. *Acta Derm Venereol* 2006; 86: 300–7.
31. Kikuchi A, Yamamoto H, Sato A, Matsumoto S. Wnt5a: its signalling, functions and implication in diseases. *Acta Physiol (Oxf)* 2012; 204: 17–33.
32. King TD, Zhang W, Suto MJ, Li Y. Frizzled7 as an emerging target for cancer therapy. *Cell Signal* 2012; 24: 846–51.
33. Gailit J, Pierschbacher M, Clark RA. Expression of functional alpha 4 beta 1 integrin by human dermal fibroblasts. *J Invest Dermatol* 1993; 100: 323–8.
34. Ong CT, Khoo YT, Mukhopadhyay A, Masilamani J, Do DV, Lim IJ, et al. Comparative proteomic analysis between normal skin and keloid scar. *Br J Dermatol* 2010; 162: 1302–15.
35. Hsieh SH, Ying NW, Wu MH, Chiang WF, Hsu CL, Wong TY, et al. Galectin-1, a novel ligand of neuropilin-1, activates VEGFR-2 signaling and modulates the migration of vascular endothelial cells. *Oncogene* 2008; 27: 3746–53.
36. Glinka Y, Stoilova S, Mohammed N, Prud'homme GJ. Neuropilin-1 exerts co-receptor function for TGF-beta-1 on the membrane of cancer cells and enhances responses to both latent and active TGF-beta. *Carcinogenesis* 2011; 32: 613–21.
37. Mogili NS, Krishnaswamy VR, Jayaraman M, Rajaram R, Venkatraman A, Korrapati PS. Altered angiogenic balance in keloids: a key to therapeutic intervention. *Transl Res* 2012; 159: 182–9.
38. Du P, Ye L, Ruge F, Yang Y, Jiang WG. Metastasis suppressor-1, MTSS1, acts as a putative tumour suppressor in human bladder cancer. *Anticancer Res* 2011; 31: 3205–12.
39. Peterfi Z, Donko A, Orient A, Sum A, Prokai A, Molnar B, et al. Peroxidase is secreted and incorporated into the extracellular matrix of myofibroblasts and fibrotic kidney. *Am J Pathol* 2009; 175: 725–35.
40. Qi B, Newcomer RG, Sang QX. ADAM19/adamalysin 19 structure, function, and role as a putative target in tumors and inflammatory diseases. *Curr Pharm Des* 2009; 15: 2336–48.
41. Rinn JL, Wang JK, Liu H, Montgomery K, van de Rijn M, Chang HY. A systems biology approach to anatomic diversity of skin. *J Invest Dermatol* 2008; 128: 776–82.
42. Park JH, Park J, Choi JK, Lyu J, Bae MG, Lee YG, et al. Identification of DNA methylation changes associated with human gastric cancer. *BMC Med Genomics* 2011; 4: 82.
43. Durani P, Bayat A. Levels of evidence for the treatment of keloid disease. *J Plast Reconstr Aesthet Surg* 2008; 61: 4–17.

Supporting Information

Additional Supporting Information may be found in the online version of this article at the publisher's web-site:

Figure S1. Heat map and list of 264 genes differentially expressed >1.3-fold in keloid fibroblasts (KF) versus normal fibroblasts (NF). Expression levels were normalized to the mean expression level in all keratinocyte and fibroblast samples. Normalized (Norm'd) and raw (shaded) expression data are shown (columns at right) for each probe set. The ratio of normalized expression in keloid vs. normal fibroblasts (KF/NF) is in bold. Heat map showing mean relative expression levels for each cell type, probe set designation, and hierarchical tree are shown at left; red represents high expression and green represents low expression.

Figure S2. Heat map and list of 216 genes differentially expressed >1.3-fold in keloid keratinocytes (KK) versus normal keratinocytes (NK). Expression levels were normalized to the mean expression level in all keratinocyte and

fibroblast samples. Normalized (Norm'd) and raw (shaded) expression data are shown (columns at right) for each probe set. The ratio of normalized expression in keloid vs. normal keratinocytes (KK/NK) is in bold. Heat map showing mean relative expression levels for each cell type, probe set designation, and hierarchical tree are shown at left; red represents high expression and green represents low expression.

Table S1. Pathways analysis of genes differentially expressed between normal and keloid fibroblasts. Shown are

the top 5 listings for each category based on *P*-values. Duplicate categories with significant overlap are not shown.

Table S2. Pathways analysis of genes differentially expressed between normal and keloid keratinocytes. Shown are the top 5 listings for each category based on *P*-values. Duplicate categories with significant overlap are not shown.